JOURNAL OF MOLECULAR SPECTROSCOPY **160,** 574–584 (1993)

Fourier Transform Infrared Emission Spectroscopy of a New $A^4\Pi_i$–$X^4\Delta_i$ System of CoO

R. S. RAM, C. N. JARMAN, AND P. F. BERNATH

Department of Chemistry, University of Arizona, Tucson, Arizona 85721; and Department of Chemistry, University of Waterloo, Waterloo, Ontario, Canada, N2L 3G1

The near-infrared emission spectrum of CoO has been recorded using a Fourier transform spectrometer. The bands observed in the region 5000–5800 cm^{-1} have been assigned to a new $A^4\Pi_i$–$X^4\Delta_i$ electronic transition. The rotational analysis of the 0–0 and 1–1 bands of the 5/2–7/2 and 3/2–5/2 subbands provide the following principal molecular constants in the $A^4\Pi_i$ state: $T_0 = 5513.9530(11)$ cm^{-1}, $A_0 = -152.3274(10)$ cm^{-1}, and $B_0 = 0.487525(83)$ cm^{-1}. Although these two subbands are free from local perturbations there is evidence of interaction with a nearby state, probably of $^4\Sigma^-$ symmetry.

INTRODUCTION

Over the past decade there has been increasing interest, both theoretical and experimental, in the electronic structure of the transition metal oxides. They are prominent in the spectra of cool stars and they are common in high-temperature terrestrial environments (*1–3*). Transition metal oxides are also important for the theoretical understanding of chemical bonding in simple metal systems. Recently, advances have been made in the ab initio calculation of the molecular properties of transition metal oxides (*1*).

The spectra of transition metal monoxides are, in general, very complex because of the presence of many closely spaced electronic states with high orbital angular momenta, large multiplicities, and large spin–orbit interactions. Due to the high density of electronic states, there are frequent perturbations. For these reasons the visible region spectra of transition metal oxides are very complex and relatively few visible transitions have been rotationally analyzed (*4–7*). The near-infrared electronic transitions of these molecules are expected to be relatively free of perturbations because of the lower density of states.

Recently, we have successfully applied Fourier transform infrared spectroscopy to the study of the near-infrared emission spectra of some transition metal oxides such as PtO (*8*) and NiO (*9*). These spectra were found to be free from local perturbations, as expected. Encouraged by these results we decided to study the infrared spectra of CoO.

There is only a limited amount of spectroscopic information on CoO available in the literature. The spectrum of CoO was first reported by Malet and Rosen (*10*) who observed many bands in the region 520–900 nm. CoO bands were also observed by chemiluminescence by McQuaid *et al.* (*11*), but they were not analyzed. Because of their great complexity, no rotational analysis of these bands was reported until 1987 when Adam *et al.* (*5*) analyzed the rotational structure of three parallel polarized ($\Delta\Omega = 0$) bands in the visible region. More than one excited state was involved because of

0022-2852/93 $5.00

massive local and global perturbations. From this analysis they concluded that the observed transitions have $\Omega'' = \frac{7}{2}$ and $\Omega'' = \frac{5}{2}$ in the ground state. These authors also determined that the $\frac{7}{2}$ state had a vibrational interval of 851.7 cm^{-1}.

The matrix infrared spectrum of CoO was studied by Green *et al.* (*12*) who obtained the vibrational constants $\omega_e = 853.75$ and $\omega_e x_e = 3.65$ cm^{-1} from $Co^{16}O$ and $Co^{18}O$. The excellent agreement between the matrix and gas-phase values suggests that $\Omega'' = \frac{7}{2}$ is the lowest spin component in the ground state supporting the assignment of the ground state as $X^4\Delta_i$.

There are only a few theoretical calculations available for transition metal oxides (*13–16*). For CoO, Krauss and Stevens (*15*) predict a $^4\Sigma^-$ ground state on the basis of their CAS-MCSCF calculations on FeO, while Dolg *et al.* (*16*) find a $^4\Delta$ state to be the lowest electronic state of CoO using Ne-like effective core potentials. Dolg *et al.* (*16*) predict that a $^4\Sigma^-$ electronic state should lie above the $^4\Delta$ ground state by an energy of 0.52 eV (4200 cm^{-1}) when relativistic effects are included.

In the present study we report the first observation of the $A^4\Pi_i$–$X^4\Delta_i$ transition of CoO in the near infrared between 5000 and 5800 cm^{-1}. The rotational analysis of the $\frac{5}{2}$–$\frac{7}{2}$ and $\frac{3}{2}$–$\frac{5}{2}$ subbands of this transition is described. Some lines of what are probably the $\frac{1}{2}$–$\frac{3}{2}$ and $-\frac{1}{2}$–$\frac{1}{2}$ subbands were also picked out but they could not be assigned because of their weak intensity. In addition, the branch intensities of the $\frac{1}{2}$–$\frac{3}{2}$ and $-\frac{1}{2}$–$\frac{1}{2}$ transitions are unusual, probably because of the presence of a nearby $^4\Sigma^-$ state.

EXPERIMENTAL DETAILS

The emission spectrum of CoO was recorded using the 1-m Fourier transform spectrometer associated with the McMath solar telescope of the National Solar Observatory at Kitt Peak. The CoO molecules were made in a Co hollow cathode discharge lamp. The new bands were observed in the 1.7- to 2.0-μm spectral region when the lamp was operated at 300 V and 350 mA current. A slow flow of 2.2 Torr of Ne and 200 mTorr of O_2 was maintained through the cathode.

The spectrometer was operated with liquid N_2-cooled InSb detectors and cooled green uranium glass filters. The use of additional room temperature Si filters limited the observed spectral region to 3300–9000 cm^{-1}. Forty-nine scans were coadded in 6 hr of integration at a resolution of 0.02 cm^{-1}.

The observed spectrum was calibrated using Ne atomic lines (*17*). The absolute accuracy of the calibration of the wavenumber scale is expected to be about ± 0.001 cm^{-1}. The lines of the $\frac{3}{2}$–$\frac{5}{2}$ subband had a full width at half-maximum of 0.025 cm^{-1} while the lines of the $\frac{5}{2}$–$\frac{7}{2}$ subband had an anomalous width of 0.050–0.140 cm^{-1}. The large width of the $\frac{5}{2}$–$\frac{7}{2}$ lines limited the accuracy to about ± 0.005 cm^{-1}.

OBSERVATION AND ANALYSIS

The observed interferograms were transformed by G. Ladd to provide the spectra in the frequency domain. A data reduction program called PC-DECOMP was used in the data reduction for the transition wavenumber determination. The peak positions were found by fitting a Voigt lineshape function to each observed spectral feature.

The new bands assigned to a $A^4\Pi_i$–$X^4\Delta_i$ transition are observed in the region 5000–5800 cm^{-1} with the strongest features (subband R heads) located at 5789.2, 5637.5, 5626.1, and 5137.5 cm^{-1}. On the basis of appearance and observed splitting of the rotational lines, these bands were tentatively identified as $\frac{5}{2}$–$\frac{7}{2}$, $\frac{3}{2}$–$\frac{5}{2}$, $\frac{1}{2}$–$\frac{3}{2}$, and $-\frac{1}{2}$–$\frac{1}{2}$ subbands, respectively. Parts of the spectra of the $\frac{5}{2}$–$\frac{7}{2}$ and $\frac{3}{2}$–$\frac{5}{2}$ subbands are given in Figs. 1 and 2.

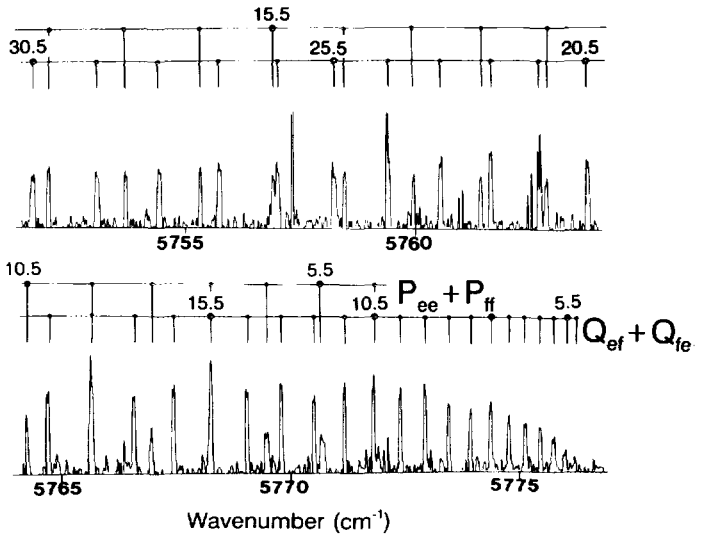

FIG. 1. A part of the spectrum of the $\frac{5}{2}$–$\frac{7}{2}$ subband of the $A^4\Pi_i$–$X^4\Delta_i$ system of CoO.

The assignment of the subbands at 5789.2 and 5637.5 cm^{-1} has been confirmed by rotational analysis. The presence of strong Q branches in the bands and the relatively weak intensity of the R branch suggest that they arise from $\Delta\Omega = -1$ transitions. The rotational analysis of the other two subbands could not be accomplished due to their weak intensity and to the absence of some of the branches necessary to form combination differences. There are no experimental data available for the $\frac{3}{2}$ and $\frac{1}{2}$ components of the $X^4\Delta_i$ state.

The band at 5789.2 cm^{-1} (Fig. 1) has been identified as the $\frac{5}{2}$–$\frac{7}{2}$ subband. The lower state combination differences in this subband match well with the data provided by Adam *et al.* (*5*) for $\Omega'' = \frac{7}{2}$. As expected, for a $\frac{5}{2}$–$\frac{7}{2}$ subband there should be P, Q, and R branches, each doubled due to the presence of Ω-doubling. The Ω-doubling splitting of a Hund's case (c) $\frac{5}{2}$ state should increase as J^5 and the splitting should not be observable except possibly at very high J.

Our observed spectrum contradicts this prediction. The lines of the $\frac{5}{2}$–$\frac{7}{2}$ transition are anomalously wide and seem to split into two partially resolved components starting at the lowest J values (Fig. 1). Adam *et al.* found no evidence for a splitting in the lower $\Omega'' = \frac{7}{2}$ state so the anomalous line shape originates from effects in the $\Omega' = \frac{5}{2}$ state.

The ^{59}Co nucleus (100% natural abundance) has a nuclear spin of $\frac{7}{2}$ and a large magnetic moment of 4.649 nuclear magnetons. We assign the anomalous lineshape in the $\frac{5}{2}$–$\frac{7}{2}$ transition to a partly resolved hyperfine structure in the $\frac{5}{2}$ state. The superposition of eight unresolved hyperfine components would result in a line with a flat top which could look "doubled" if the spectrum was noisy. This explanation is not entirely satisfactory because a Hund's case (a) $^4\Pi$ state should follow case a_β hyperfine coupling (*18*). The $A^4\Pi_{5/2}$ state should have a larger hyperfine splitting than the $^4\Pi_{3/2}$ state, in agreement with the data. The hyperfine splitting within the $^4\Pi_{5/2}$ state should decrease as $1/J$ as J increases, but this is not entirely in agreement with the experimental data. At low J the linewidth in the Q branch decreases from 0.090 cm^{-1} at $J = 6.5$ to 0.060 cm^{-1} at $J = 13.5$, remains constant until about $J = 30.5$, and

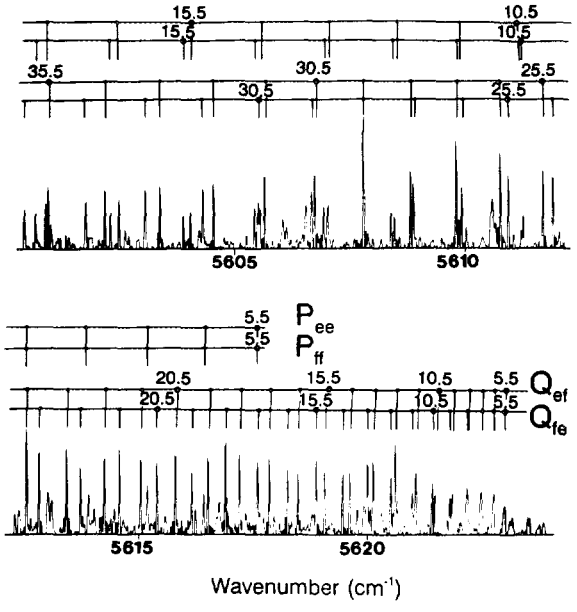

FIG. 2. A part of the spectrum of the $\frac{3}{2}$–$\frac{5}{2}$ subband of the $A^4\Pi_i$–$X^4\Delta_i$ system of CoO.

then increases slowly up to 0.100 cm^{-1}. A similar pattern is observed in the P branch. The increase at high J seems to be the result of Ω-doubling while the constant linewidth may be due to the effects of electron spin uncoupling. For complete spin uncoupling the hyperfine coupling case would be $b_{\beta J}$. For $b_{\beta J}$ coupling the hyperfine splitting decreases as J increases but approaches a constant value at high J.

The band at 5637.5 cm^{-1} has been assigned as the $\frac{3}{2}$–$\frac{5}{2}$ subband. The structure of this band shows the presence of two P, two Q, and two R branches (Fig. 2). The two Ω-doubling components are well resolved (except for the first few J values) and their splitting increases as J^3, as expected if the Ω-doubling is present almost entirely in the $\Omega' = \frac{3}{2}$ state. The analysis of this band was straightforward, using the lower state combination differences reported by Adam *et al.* (*5*). In addition, the lower state combination differences formed between the R_{ee} and P_{ee} branches are identical within experimental error to those formed between the R_{ff} and P_{ff} branches, confirming that the Ω-doubling arises solely from the excited $\frac{3}{2}$ state.

The rotational structure of the 1–1 bands of both subbands is similar to those in the 0–0 bands. The observed transition wavenumbers in each band were fitted to the usual N^2 Hamiltonian for $^4\Pi$ and $^4\Delta$ states as given by Brown *et al.* (*19*). An explicit listing of the matrix elements are provided by Brown *et al.* for a $^4\Delta$ state (*20*), while the $^4\Pi$ matrix elements are given by Brown and Merer (*21*). Additional centrifugal distortion terms q_D, p_D, and o_D were needed in the $A^4\Pi_i$ state in order to obtain a satisfactory fit. They were derived by matrix multiplication. An explicit listing of the matrix elements for a $^4\Pi$ state, including the additional centrifugal distortion terms, is provided in Table I.

The molecular parameters T_0, A_0, A_{D0}, B_0, D_0, q_0, p_0, q_{D0}, p_{D0}, and λ_{D0} in the $A^4\Pi_i$ state and B_0, D_0, q_0, p_0, and λ_{D0} in the $X^4\Delta$ state were varied in the fitting of the 0–0 band. The lower state parameters A_0 and λ_0 were held fixed at the values

TABLE I

Matrix Elements for a $^4\Pi$ N^2 Hamiltonian in a Hund's Case (a) Basis (Upper and Lower Sign Choices Refer to e and f Levels, Respectively)

$\left\|-\frac{1}{2}\right\rangle$	$\left\|\frac{1}{2}\right\rangle$	$\left\|\frac{3}{2}\right\rangle$	$\left\|\frac{5}{2}\right\rangle$
$-3A/2+(B-3A_D/2+2\lambda_D)(z+2)$ $+2\lambda-3\gamma-D(z^2+7z+4)$ $\pm3\sqrt{z}(o_D+p_D+q_D)$	$-\sqrt{3}\begin{pmatrix}\sqrt{z}(B-\gamma/2-A_D-2D(z+3))\\ \pm\begin{pmatrix}o+p+q+p_D(4z+5)/2\\ +q_D(3z+2)+o_D(z+3)\end{pmatrix}\end{pmatrix}$	$\frac{\sqrt{3(z-1)}}{2}\begin{bmatrix}-4\sqrt{z}D\pm\{2q+2o_D+p\\ +p_D(z+4)+q_D(3z+4)\}\end{bmatrix}$	$\mp\frac{\sqrt{(z-1)(z-4)}}{2}\begin{pmatrix}q+q_D(z+2)\\ +3/2\,p_D\end{pmatrix}$
	$-A/2+(B-A_D/2-2\lambda_D)(z+4)$ $-2\lambda-4\gamma-D(z^2+15z+12)$ $\pm\sqrt{z}\begin{pmatrix}3o_D+p+p_D(z+7)\\ +2q+q_D(3z+10)\end{pmatrix}$	$-2\sqrt{z-1}\begin{pmatrix}B-\gamma/2-2\lambda_D-2D(z+3)\\ \pm\frac{\sqrt{z}}{4}\begin{pmatrix}q+7/2\,p_D\\ +q_D(z+10)\end{pmatrix}\end{pmatrix}$	$\frac{\sqrt{3(z-1)(z-4)}}{2}\begin{pmatrix}-4D\\ \pm q_D\sqrt{z}\end{pmatrix}$
		$A/2+(B+A_D/2-2\lambda_D)(z+2)$ $-2\lambda-3\gamma-D(z^2+11z-12)$ $\pm q_D\sqrt{z}(z-1)$	$-3\sqrt{z-4}\begin{pmatrix}B-\gamma/2+A_D\\ -2D(z-1)\end{pmatrix}$
			$3A/2+(B+3A_D/2+2\lambda_D)(z-4)$ $+2\lambda-D(z^2-5z+4)$

estimated from the data provided by Merer *et al.* (*22*). Merer and co-workers measured the $\Omega'' = \frac{7}{2}$ to $\Omega'' = \frac{5}{2}$ interval to be 304.321 cm^{-1} and the $\Omega'' = \frac{5}{2}$ to $\Omega'' = \frac{3}{2}$ interval as 337.5 cm^{-1}. From these intervals the constants $A = -168.75$ cm^{-1} and $\lambda = 8.2947$ cm^{-1} were determined and held fixed in our fits.

For the 1–1 band the A_{D1} constant could not be determined with sufficient precision; therefore this parameter was held fixed at the value determined for the $v = 0$ level. The observed transition wavenumbers for the 0–0 band of CoO are given in Table II and those for the 1–1 band are given in Table III. The rotational constants for the $v = 0$ and $v = 1$ levels of the $X^4\Delta_i$ state are reported in Table IV and the corresponding values for the $A^4\Pi_i$ state are given in Table V. It should be noted that both the $A^4\Pi_i$ and the $X^4\Delta_i$ states display considerable Hund's case (c) tendencies. This means that the spectroscopic constants reported in Tables IV and V are only "effective" parameters. The values are greatly distorted by interaction between the various low-lying electronic states.

DISCUSSION

The rotational constants of Tables IV and V have been used to evaluate the equilibrium molecular constants for the ground and the excited states (Table VI). The B_e and α_e values for the $X^4\Delta_i$ state are 0.505192(20) and 0.003991(37) cm^{-1}, while the corresponding values for the $A^4\Pi_i$ state are 0.49029(11) and 0.00552(15) cm^{-1}, respectively. The equilibrium bond lengths for the ground and excited states have been determined as 1.628626(32) and 1.65319(18) Å from the equilibrium B_e values.

The ground states of most of the transition metal oxides have been relatively well characterized but very little is known about the excited electronic states. Part of the problem is associated with experimental limitations since it is difficult to obtain strong spectra for d–d transitions of the $3d$ transition metal oxides. In addition, these spectra are often perturbed. Part of the problem also lies with theory since in these molecules the molecular orbitals derived from the metal $3d$ and $4s$ atomic orbitals as well as the $2p$ oxygen atomic orbital are almost degenerate. This makes it very difficult to calculate the properties of the numerous excited electronic states.

The ab initio theoretical work of Krauss and Stevens (*15*) predicted a $^4\Sigma^-$ state arising from the $\sigma\delta^4\pi^2$ configuration to be the ground state of this molecule. This

TABLE II

Observed Transition Wavenumbers (in cm^{-1}) of the 0–0 Band of the $A^4\Pi_i$–$X^4\Delta_i$ system of CoO

3/2 - 5/2 Subband												
J	R_{ee}	O-C	R_{ff}	O-C	Q_{ef}	O-C	Q_{fe}	O-C	P_{ee}	O-C	P_{ff}	O-C
3.5									5619.917	-0	5619.917	1
4.5									5618.776	-9	5618.776	-6
5.5	5629.270	15					5622.952	10	5617.629	11		
6.5	5629.998	5					5622.707	4	5616.409	-6	5616.409	4
7.5	5630.712	18					5622.433	6	5615.170	-7	5615.170	9
8.5	5631.360	-0			5622.153	6	5622.123	10	5613.894	-8	5613.894	15
9.5	5631.997	5			5621.811	3	5621.762	-0	5612.571	-23	5612.571	10
10.5					5621.430	-4	5621.375	2	5611.251	1	5611.206	1
11.5	5633.150	2	5633.057	8	5621.027	2	5620.947	-0	5609.863	-8	5609.804	-7
12.5	5633.684	9	5633.547	-4	5620.581	0	5620.485	2	5608.458	1	5608.379	-1
13.5	5634.177	11	5634.011	-3	5620.102	-1	5619.979	-0	5607.010	0	5606.917	6
14.5	5634.625	3	5634.439	0	5619.588	-2	5619.437	-1	5605.529	2	5605.406	2
15.5	5635.048	4	5634.825	0	5619.041	-2	5618.856	-3	5604.008	-2	5603.859	0
16.5	5635.429	-2	5635.171	-0	5618.459	-1	5618.239	-2	5602.459	-0	5602.276	0
17.5	5635.781	-2	5635.478	-1	5617.842	-3	5617.586	2	5600.871	-3	5600.657	3
18.5	5636.098	-4	5635.737	-11	5617.193	-0	5616.888	-1	5599.251	-3	5598.992	-2
19.5	5636.381	-4	5635.978	1	5616.508	-0	5616.147	-8	5597.602	2	5597.297	1
20.5	5636.636	2	5636.164	-3	5615.790	1	5615.381	0	5595.911	-2	5595.558	-1
21.5	5636.847	-2	5636.317	-1	5615.032	-4	5614.569	-0	5594.189	-3	5593.784	0
22.5	5637.028	-1	5636.430	2	5614.247	-2	5613.719	2	5592.435	-1	5591.969	-1
23.5	5637.177	2	5636.494	-6	5613.424	-4	5612.826	-0	5590.648	0	5590.116	-0
24.5	5637.281	-5			5612.571	-2	5611.897	0	5588.824	-1	5588.225	1
25.5	5637.368	5			5611.681	-3	5610.927	1	5586.968	-1	5586.298	4
26.5					5610.759	-2	5609.919	2	5585.080	0	5584.322	-1
27.5			5636.381	-2	5609.804	1	5608.869	1	5583.155	-2	5582.315	1
28.5			5636.247	-7	5608.811	-1	5607.783	4	5581.198	-2	5580.270	4
29.5	5637.326	-2	5636.076	-8	5607.783	-4	5606.652	1	5579.210	0	5578.181	3
30.5	5637.226	-8	5635.875	2	5606.726	-2	5605.487	4	5577.189	2	5576.052	0
31.5	5637.105	1	5635.608	-15	5605.634	-2	5604.277	3	5575.130	0	5573.891	5
32.5	5636.936	-4	5635.341	9	5604.509	-1	5603.029	2	5573.040	0	5571.681	0
33.5	5636.738	-5	5634.998	-1	5603.348	-2	5601.737	-1	5570.917	0	5569.436	1
34.5	5636.516	6	5634.625	-2	5602.155	-1	5600.415	5	5568.761	1	5567.148	-3
35.5	5636.247	4	5634.213	-1	5600.926	-2	5599.045	3	5566.583	13	5564.834	6
36.5	5635.939	-1	5633.762	2	5599.663	-2	5597.641	8			5562.456	-9
37.5	5635.608	5	5633.267	2	5598.367	-2	5596.190	5	5562.091	1	5560.070	8
38.5	5635.231	-0			5597.037	-2	5594.697	1	5559.802	2	5557.615	-5
39.5	5634.825	0	5632.155	2	5595.674	-1	5593.161	-6	5557.476	-1	5555.128	-11
40.5	5634.388	5	5631.534	-1	5594.276	0	5591.597	-1	5555.128	8	5552.600	-19
41.5					5592.845	2	5589.994	5	5552.732	2		
42.5	5633.398	5			5591.375	-1	5588.336	-3	5550.309	3		
43.5	5632.850	5			5589.870	-3	5586.658	8				
44.5	5632.268	7			5588.336	-1	5584.906	-14	5545.368	11		
45.5	5631.647	5			5586.765	-1	5583.155	5				
46.5	5630.991	5			5585.156	-4	5581.336	-3	5540.277	5		
47.5					5583.514	-6	5579.492	3	5537.680	1		
48.5					5581.839	-4	5577.578	-20	5535.051	-0		
49.5					5580.131	-1	5575.656	-10	5532.393	3		
50.5					5578.383	-1	5573.700	5	5529.699	5		
51.5					5576.597	-5	5571.681	-2	5526.962	-1		
52.5					5574.782	-1	5569.612	-19	5524.193	-5		
53.5					5572.915	-14	5567.516	-23	5521.395	-2		
54.5					5571.033	-5	5565.409	3	5518.563	1		
55.5					5569.105	-4	5563.239	6	5515.681	-10		
56.5					5567.148	4	5561.023	3	5512.769	-16		
57.5					5565.152	9	5558.772	5				
58.5					5563.099	-4	5556.467	-5	5506.856	-9		
59.5					5561.023	-3	5554.139	2	5503.851	1		
60.5					5558.919	8	5551.766	3	5500.794	-5		
61.5					5556.762	4						

result is not consistent with the experimental measurements (*5, 13*). More recently, Dolg *et al.* (*16*) predicted a $^4\Delta$ state to be the lowest electronic state of CoO arising from the $\sigma^2\delta^3\pi^2$ configuration and suggested that the $^4\Sigma^-$ state arising from the $\sigma\delta^4\pi^2$ configuration should lie at about 0.52 eV above the ground $^4\Delta$ state.

TABLE II—*Continued*

5/2 - 7/2 Subband												
J	R_{ee}	O-C	R_{ff}	O-C	Q_{ef}	O-C	Q_{fe}	O-C	P_{ee}	O-C	P_{ff}	O-C
4.5					5776.222	1	5776.222	1				
5.5	5782.270	-2	5782.270	-2	5776.014	2	5776.014	2	5770.708	-8	5770.708	-8
6.5	5782.983	-5	5782.983	-5	5775.767	1	5775.767	1	5769.502	-5	5769.502	-5
7.5	5783.675	9	5783.675	9	5775.479	-3	5775.479	-3	5768.277	18	5768.277	18
8.5					5775.156	-2	5775.156	-2	5766.975	1	5766.975	1
9.5	5784.907	1	5784.907	1	5774.799	1	5774.799	1	5765.654	3	5765.654	3
10.5	5785.467	-2	5785.467	-2	5774.403	4	5774.403	4	5764.294	5	5764.294	5
11.5	5785.990	-3	5785.990	-4	5773.963	2	5773.963	2	5762.887	-3	5762.887	-3
12.5	5786.480	1	5786.480	1	5773.487	2	5773.487	2	5761.453	0	5761.453	0
13.5	5786.922	-3	5786.922	-4	5772.966	-5	5772.966	-5	5759.977	-0	5759.977	-0
14.5	5787.335	2	5787.335	2	5772.420	2	5772.420	2	5758.462	-1	5758.462	-1
15.5	5787.706	3	5787.706	3	5771.833	7	5771.833	7	5756.903	-8	5756.903	-9
16.5	5788.038	6	5788.038	5	5771.198	2	5771.198	1	5755.320	-0	5755.320	-1
17.5	5788.321	-2	5788.321	-3	5770.529	2	5770.529	2	5753.688	-4	5753.688	-4
18.5	5788.576	2	5788.576	1	5769.818	-0	5769.818	-1	5752.021	-3	5752.021	-4
19.5					5769.072	1	5769.072	-0	5750.297	-20	5750.297	-21
20.5					5768.277	-8	5768.277	-9	5748.570	-2	5748.570	-3
21.5	5789.115	26	5789.115	25	5767.464	5	5767.464	3	5746.783	-5	5746.783	-6
22.5	5789.207	26	5789.207	24	5766.595	1	5766.595	-1	5744.967	3	5744.967	1
23.5	5789.250	17	5789.250	15	5765.690	1	5765.690	-2	5743.103	1	5743.103	-1
24.5					5764.747	3	5764.747	1	5741.204	3	5741.204	1
25.5					5763.762	3	5763.762	-1	5739.261	2	5739.261	-1
26.5					5762.740	6	5762.740	2	5737.276	-2	5737.276	-5
27.5	5789.065	31	5789.065	26	5761.676	7	5761.676	3	5735.260	2	5735.260	-1
28.5	5788.900	18	5788.900	12	5760.570	7	5760.570	2	5733.202	5	5733.202	1
29.5	5788.700	12	5788.700	6					5731.099	3	5731.099	-2
30.5	5788.449	-4	5788.449	-11	5758.234	7	5758.234	0				
31.5	5788.168	-8	5788.168	-16	5757.004	6	5757.004	-2				
32.5	5787.837	-20	5787.837	-29	5755.736	8	5755.736	-0				
33.5	5787.496	0	5787.496	-9	5754.422	6	5754.422	-3				
34.5	5787.078	-13	5787.078	-24	5753.065	3	5753.065	-8				
35.5					5751.676	10	5751.676	-2				
36.5	5786.150	-4	5786.150	-17	5750.214	-13	5750.214	-27				
37.5	5785.628	7	5785.628	-6	5748.748	2	5748.748	-13				
38.5	5785.044	0	5785.044	-14	5747.232	9	5747.232	-7				
39.5	5784.428	5	5784.428	-10	5745.665	9	5745.665	-8				
40.5			5783.784	12	5744.041	-4						

The configuration of the excited $A^4\Pi_i$ state is more difficult to predict but the spectra contain some important clues. The relatively small hyperfine structure is consistent with closed σ orbitals. Any open $s\sigma$ orbitals would give rise to substantial hyperfine structures as are found for many other transition metal oxides (*1*) and in the higher excited states of CoO (*5*). The $A^4\Pi_i$ state must also have more than half filled δ and/or π orbitals in order to be inverted. The $\sigma^2\delta^2\pi^3$ configuration is consistent with this information and gives rise to $^4\Pi_i$, $^2\Pi_i$ (two), $^2\Phi_i$, and ^2H_i states. By Hund's rule the $^4\Pi_i$ state would lie lowest in energy but, as usual, the single configuration approximation may not be very reliable for the excited CoO states. There are also Hund's case (c) tendencies in the excited states of CoO, as evidenced by the intervals between the spin components.

The $A^4\Pi$–$X^4\Delta$ transition of CoO thus corresponds to the promotion $\delta \rightarrow \pi$. The other likely single electron promotion from the ground state configuration $\sigma^2\delta^3\pi^2$ is $\sigma \rightarrow \pi$, which would give a $\sigma^1\delta^2\pi^3$ configuration. The $\sigma^1\delta^2\pi^3$ configuration would also give a $^4\Pi_i$ state but with an unpaired electron in a metal $4s\sigma$ orbital; the hyperfine structure is expected to be larger than what is found experimentally. It is likely that both the $\sigma^1\delta^3\pi^3$ and the $\sigma^2\delta^2\pi^3$ configurations make contributions to the electronic wavefunction of the $A^4\Pi$ state but with a larger contribution from $\sigma^2\delta^2\pi^3$.

TABLE III

Observed Transition Wavenumbers (in cm^{-1}) of the 1–1 Band of the $A^4\Pi_i$–$X^4\Delta_i$ System of CoO

3/2 - 5/2 Subband

J	R_{ee}	O-C	Q_{ef}	O-C	Q_{fe}	O-C	P_{ee}	O-C	P_{ff}	O-C
5.5					5569.058	-10				
6.5					5568.821	-2	5562.590	-4		
7.5	5576.719	-11	5568.578	15	5568.539	-1	5561.347	-9	5561.347	7
8.5	5577.368	-11	5568.258	8	5568.232	15	5560.070	-13	5560.070	10
9.5	5577.993	1	5567.903	1			5558.772	-2	5558.737	-4
10.5	5578.567	-1	5567.516	-1	5567.456	-1	5557.423	-5	5557.383	-0
11.5			5567.099	2	5567.020	2	5556.049	2	5555.968	-18
12.5	5579.614	1	5566.640	-0	5566.548	8	5554.634	4	5554.559	8
13.5	5580.080	-1	5566.145	-4	5566.032	8	5553.177	-0		
14.5	5580.512	-1	5565.618	-3	5565.469	1	5551.697	9	5551.561	-2
15.5	5580.911	0	5565.058	1	5564.867	-5	5550.167	2	5550.009	-3
16.5	5581.277	5					5548.603	-2		
17.5	5581.595	-1	5563.819	-4	5563.563	2				
18.5	5581.885	-1	5563.155	1	5562.848	2	5545.368	-13		
19.5	5582.118	-21	5562.456	8	5562.091	0	5543.704	-10		
20.5			5561.706	-1	5561.297	1	5542.015	0		
21.5			5560.928	-3	5560.460	1	5540.277	-2		
22.5			5560.118	-1	5559.582	-1	5538.511	2	5538.040	1
23.5			5559.271	-1	5558.668	2	5536.699	-5	5536.170	2
24.5			5558.389	-1	5557.706	-2	5534.863	0	5534.261	3
25.5			5557.476	4	5556.707	-3	5532.991	3	5532.313	6
26.5			5556.518	-1	5555.670	1	5531.079	0	5530.316	-0
27.5			5555.527	-3	5554.582	-6	5529.124	-10		
28.5			5554.504	-3	5553.454	-12	5527.155	1	5526.219	5
29.5			5553.454	6	5552.302	-0	5525.141	1	5524.102	0
30.5			5552.354	1	5551.097	-1	5523.091	-0	5521.951	2
31.5			5551.222	-2	5549.848	-4	5521.005	-2	5519.758	2
32.5			5550.064	5	5548.562	-1	5518.886	-3	5517.509	-13
33.5			5548.862	5			5516.735	-0	5515.244	-2
34.5					5545.869	6	5514.549	1	5512.928	-3
35.5					5544.455	5	5512.325	-0		
36.5							5510.067	0		
37.5			5543.704	8			5507.776	2		
38.5			5542.313	-3						
39.5										
40.5			5539.439	-6						
41.5			5537.957	2						
42.5			5536.429	1						

5/2 - 7/2 Subband

J	R_{ee}	O-C	R_{ff}	O-C	Q_{ef}	O-C	Q_{fe}	O-C	P_{ee}	O-C	P_{ff}	O-C
5.5					5715.828	-6	5715.828	-6	5710.601	-4	5710.601	-4
6.5					5715.571	13	5715.571	13	5709.354	-24	5709.354	-24
7.5	5723.305	-15	5723.305	-15	5715.253	13	5715.253	13	5708.097	-13	5708.097	-13
8.5	5723.911	3	5723.911	3	5714.868	-11	5714.868	-11	5706.773	-26	5706.773	-26
9.5	5724.470	16	5724.470	16	5714.467	-8	5714.467	-8				
10.5	5724.982	26	5724.982	26	5714.028	1	5714.028	1	5704.064	15	5704.064	15
11.5	5725.418	3	5725.418	3	5713.529	-8	5713.529	-8	5702.614	5	5702.614	5
12.5	5725.826	-4	5725.826	-4	5713.007	3	5713.007	3	5701.114	-12	5701.114	-12
13.5					5712.432	6	5712.432	6	5699.610	10	5699.610	10
14.5	5726.555	28	5726.555	28	5711.798	-8	5711.798	-8				
15.5	5726.811	2	5726.811	1	5711.142	2	5711.142	2				
16.5	5727.076	29	5727.076	29	5710.409	-22	5710.409	-22	5694.777	16	5694.777	16
17.5	5727.275	36	5727.276	35	5709.678	1	5709.678	0	5693.069	9	5693.069	8
18.5					5708.876	-2	5708.876	-3	5691.312	-3	5691.312	-3
19.5					5708.047	13	5708.047	12	5689.522	-4	5689.522	-4
20.5					5707.148	3	5707.148	2	5687.686	-5	5687.686	-6
21.5					5706.205	-5	5706.205	-6	5685.818	7	5685.818	6
22.5					5705.237	7	5705.237	6				
23.5					5704.191	-11	5704.191	-12				
24.5					5703.131	3	5703.131	1				
25.5					5701.997	-9	5701.997	-11				
26.5					5700.841	3	5700.841	1				
27.5					5699.610	-12	5699.610	-14				
28.5												
29.5					5697.036	-6	5697.036	-9				
30.5					5695.676	-4	5695.676	-7				
31.5					5694.280	13	5694.280	10				
32.5					5692.806	3	5692.806	-1				
33.5					5691.312	22	5691.312	19				
34.5					5689.745	20	5689.745	17				
35.5					5688.111	3	5688.111	1				
36.5					5686.400	-39						
37.5					5684.716	-1	5684.716	-2				

TABLE IV

Spectroscopic Constants (in cm^{-1}) for the $X\,^4\Delta_i$ State of CoO

Constants[a]	v = 0	v = 1
A_v	-168.75[b]	-168.75[c]
B_v	0.5031969(81)	0.499206(36)
$10^7 \times D_v$	6.480(35)	5.32(40)
$10^6 \times q_v$	0.604(12)	1.49(12)
$10^4 \times p_v$	1.192(25)	2.98(25)
λ_v	8.2947[b]	8.2947[c]
$10^4 \times \lambda_{Dv}$	-1.100(21)	-0.88(12)

[a]One standard deviation error is given in parentheses.
[b]Fixed at the values calculated from the data provided by Merer (22).
[c]Fixed at the value for v = 0.

Some information about the nearby $^4\Sigma^-$ state is available from the large Ω-doubling observed in the $\Omega' = \frac{3}{2}$ component of the $A\,^4\Pi$ state. If the pure precession approximation is used for the interaction of the $^4\Pi$ state with the $^4\Sigma^-$ state (7), then

$$p = -2\langle {}^4\Pi | AL^+ | {}^4\Sigma^- \rangle \langle {}^4\Pi | BL^+ | {}^4\Sigma^- \rangle / \Delta E_{\Pi\Sigma} = -2[l(l+1)AB]/\Delta E_{\Pi\Sigma}$$

and

$$q = -2|\langle {}^4\Pi | BL^+ | {}^4\Sigma^- \rangle|^2 / \Delta E_{\Pi\Sigma} = -2B^2 l(l+1)/\Delta E_{\Pi\Sigma}.$$

If $l = 2$ for a d orbital, $A = -152.3$ cm^{-1}, $B = 0.4907$ cm^{-1}, and the $^4\Sigma^-$ state is assumed to be 1200 cm^{-1} below the $A\,^4\Pi$ state, then $p = 0.74$ cm^{-1} and $q = -2.4 \times$

TABLE V

Spectroscopic Constants (in cm^{-1}) for the $A\,^4\Pi_i$ State of CoO

Constants[a]	v = 0	v = 1
T_v	5513.9530(11)	5463.2242(24)
A_v	-152.3274(10)	-158.5723(21)
$10^4 \times A_{Dv}$	-6.03(86)	-6.03[b]
B_v	0.487525(83)	0.48201(13)
$10^6 \times D_v$	1.0240(45)	1.312(44)
$10^3 \times q_v$	4.73(16)	4.38(62)
p_v	0.728(14)	0.732(59)
$10^6 \times q_{Dv}$	-0.983(12)	-2.18(15)
$10^4 \times p_{Dv}$	-0.973(12)	-2.16(13)
$10^4 \times \lambda_{Dv}$	-2.34(28)	-6.74(53)

[a]One standard deviation error is given in parentheses.
[b]Fixed at the value for v = 0.

TABLE VI

Equilibrium Constants (in cm^{-1}) for the $A^4\Pi_i$ and $X^4\Delta_i$ States of CoO

Constants[a]	$A^4\Pi_i$	$X^4\Delta_i$
B_e	0.49029(11)	0.505192(20)
α_e	0.00552(15)	0.003991(37)
r_e(Å)	1.65319(18)	1.628626(32)

[a]One standard deviation error is given in parentheses.

10^{-3} cm^{-1}. The observed values are $p = 0.7329$ cm^{-1} and $q = 4.79 \times 10^{-3}$ cm^{-1}. The agreement in magnitude is satisfactory suggesting that a nearby $^4\Sigma^-$ state is responsible for the large Ω-doubling in the $A^4\Pi$ state. The single configuration approximation and the pure precession relationships are not expected to be very reliable so the disagreement between the predicted and the observed sign of q is not surprising.

The absolute signs of the two Ω-doubling constants p and q cannot be determined from our fits. Exchanging the e and f parity labels simply changes the signs of the A state Ω-doubling constants. The variance of the fit is also nearly the same, increasing to 0.59 from 0.56 when p and q are negative. We therefore arbitrarily choose p and q to be positive, consistent (for the p constant) with the $^4\Sigma^-$ state lying below the $A^4\Pi$ state. Note that the values of p and q are so large that they also affect the value of the rotational constant B in the $A^4\Pi$ state.

The weak intensity and anomalous relative intensity of the branches in the $A^4\Pi_{1/2}$–$X^4\Delta_{3/2}$ and $A^4\Pi_{-1/2}$–$X^4\Delta_{1/2}$ subbands are also consistent with a nearby $^4\Sigma^-$ state. Direct mixing of the electronic wavefunctions of the $^4\Sigma_{1/2}$ spin component with the $^4\Pi_{1/2}$ and $^4\Pi_{-1/2}$ spin components through the $\hat{l}_+\hat{s}_-$ part of the spin–orbit operator is possible. These problems, combined with the absence of ground state combination differences for the $X^4\Delta_{3/2}$ and $X^4\Delta_{1/2}$ spin components, prevented any detailed analysis of the $A^4\Pi_{1/2}$–$X^4\Delta_{3/2}$ and $A^4\Pi_{1/2}$–$X^4\Delta_{3/2}$ subbands.

CONCLUSION

This work is the first gas-phase investigation of the near-infrared electronic spectra of CoO. A new $A^4\Pi_i$–$X^4\Delta_i$ electronic transition has been identified. Rotational analysis of the 0–0 and 1–1 bands of the $\frac{5}{2}$–$\frac{7}{2}$ and $\frac{3}{2}$–$\frac{5}{2}$ subbands was carried out. The lower state of this transition is the $X^4\Delta_i$ state arising from $\sigma^2\delta^3\pi^2$ configuration as discussed in detail by Adam *et al.* (*5*).

The near-infrared bands investigated in the present study of CoO are free from local perturbations as were the transitions of PtO (*8*) and NiO (*9*). Similar infrared electronic transitions for other transition metal oxides may also avoid the spectral congestion and extensive perturbations present in the visible spectra.

ACKNOWLEDGMENTS

We thank J. Wagner, C. Plymate, and G. Ladd for help in acquiring the spectra. The National Solar Observatory is operated by the Association of Universities for Research in Astronomy, Inc., under contract with the National Science Foundation. This work was supported by the Petroleum Research Fund, administered by the American Chemical Society. Some support was also provided by the Natural Sciences and

Engineering Research Council of Canada. We thank A. Merer for helpful discussions and communication of his unpublished results on CoO.

RECEIVED: March 19, 1993

REFERENCES

1. A. J. MERER, *Annu. Rev. Phys. Chem.* **40,** 407–438 (1989).
2. D. N. DAVIS, *Astrophys. J.* **106,** 28–75 (1947).
3. H. SPINRAD AND R. F. WING, *Annu. Rev. Astron. Astrophys.* **7,** 269–302 (1969).
4. V. I. SRDANOV AND D. O. HARRIS, *J. Chem. Phys.* **89,** 2748–2753 (1988).
5. A. G. ADAM, Y. AZUNA, J. A. BARRY, G. HUANG, M. P. J. LYNE, A. J. MERER, AND J. O. SCHRÖDER, *J. Chem. Phys.* **86,** 5231–5238 (1987).
6. A. S.-C. CHEUNG, W. ZYRNICKI, AND A. J. MERER, *J. Mol. Spectrosc.* **104,** 315–336 (1984).
7. A. S.-C. CHEUNG, A. W. TAYLOR, AND A. J. MERER, *J. Mol. Spectrosc.* **92,** 391–409 (1982).
8. C. I. FRUM, R. ENGLEMAN, JR., AND P. F. BERNATH, *J. Mol. Spectrosc.* **150,** 566–575 (1991).
9. R. S. RAM AND P. F. BERNATH, *J. Mol. Spectrosc.* **155,** 315–325 (1992).
10. L. MALET AND B. ROSEN, *Bull. Soc. R. Sci. Liége* **14,** 382–389 (1945).
11. M. J. MCQUAID, K. MORRIS, AND J. L. GOLE, *J. Am. Chem. Soc.* **110,** 5280–5285 (1988).
12. D. W. GREEN, G. T. REEDY, AND J. C. KAY, *J. Mol. Spectrosc.* **78,** 257–266 (1979).
13. S. P. WALCH AND W. A. GODDARD, *J. Mol. Spectrosc.* **100,** 1338–1348 (1978).
14. C. W. BAUSCHLICHER, JR., C. J. NELIN, AND P. S. BAGUS, *J. Chem. Phys.* **82,** 3265–3276 (1985).
15. M. KRAUSS AND W. J. STEVENS, *J. Chem. Phys.* **82,** 5584–5596 (1985).
16. M. DOLG, U. WEDIG, H. STOLL, AND H. PREUSS, *J. Chem. Phys.* **86,** 2123–2131 (1987).
17. B. A. PALMER AND R. ENGLEMAN, Atlas of the Thorium Spectrum, unpublished, Los Alamos National Laboratory, Los Alamos, 1983.
18. T. M. DUNN, *in* "Molecular Spectroscopy: Modern Research" (K. Narahari Rao and C. W. Mathews, Eds.), Vol. 1, Academic Press, New York, 1972.
19. J. M. BROWN, E. A. COLBOURN, J. K. G. WATSON, AND F. D. WAYNE, *J. Mol. Spectrosc.* **74,** 425–436 (1979).
20. J. M. BROWN, A. S.-C. CHEUNG, AND A. J. MERER, *J. Mol. Spectrosc.* **124,** 464–475 (1987).
21. J. M. BROWN AND A. J. MERER, *J. Mol. Spectrosc.* **74,** 488–494 (1979).
22. A. J. MERER, private communication.